GSA Data Repository 2018365

Reassessing the dissolved molybdenum isotopic composition of ocean inputs: The effect of chemical weathering and groundwater

Elizabeth K. King, and Julie C. Pett-Ridge

College of Earth, Ocean, and Atmospheric Sciences, Oregon State University, Corvallis, Oregon 97331, USA

Table DR1

Geochemical and Mo data for groundwater and river samples from the Hawaiian Islands and Critical Zone Observatories

Sample Location	Sample Name	Sample Type	Dominant rock type, soil order	Duration of weathering[a]	Discharge	Mo Discharge[b]	MAP[c]	Mo	δ^{98}Mo
				kyr	$m^3\ s^{-1}$	mol Mo yr^{-1}	mm yr^{-1}	nM	‰
Hawai'i									
Kona Region	PW1	groundwater	Basalt, Andisols	5–10	245.1	1.72E+05	385	22.23	0.45
	PW3	groundwater		5–10	--	--	385	19.06	--
	PW4	groundwater		5–10	245.1	1.67E+05	385	21.61	0.25
	PW7	groundwater		5–10	245.1	3.15E+05	385	40.82	0.36
	IW5	groundwater		5–10	--	--	376	50.62	--
	Puu Lani	groundwater		5–10	245.1	2.89E+05	592	37.41	0.51
	Pu'u Wa'awa'a	groundwater		5–10	--	--	672	29.58	--
	Ke'ei	groundwater		5–10	245.1	8.83E+04	1252	11.43	0.34
	Kalaoa	groundwater		5–10	245.1	1.31E+05	955	16.92	0.44
	Honokōhau	groundwater		5–10	245.1	1.27E+06	1000	164.11	0.44
Hilo-Hamakua Coast	Makahiloa	stream	Basalt, Andisols	64–300	0.0	7.13E-02	4663	0.15	0.24
	Pāhale	stream		64–300	--	--	4026	0.09	--
	Manoloa	stream		64–300	0.0	2.19E-02	5205	0.14	0.61
	Manowai'ōpae	stream		64–300	--	--	4689	0.17	--
	Kapue	stream		64–300	0.5	2.25E+00	5696	0.14	0.88
	Honoli'i	stream		64–300	1.1	3.49E+00	5751	0.10	-0.28
	Kolekole	stream		64–300	0.5	6.90E+01	6426	4.68	0.04
Kohala Peninsula	Pololu 1	headwater stream	Basalt, Andisols	400	64.8	3.15E+03	4000	1.54	0.50
	Pololou 2	stream		400	--	--	4000	0.60	--
	WP87	stream		400	64.8	2.40E+03	4000	1.18	0.32
	Waipi'o	stream		400	0.1	1.56E+01	4000	7.49	0.24
Maui, Hawai'i									
	MCG site 3	stream	Basalt, Andisols	410	--	--	2800	0.13	0.74

	MCG site 5	stream	Basalt, Inceptisols	410	--	--	5050	0.17	-0.22
Kaua'i, Hawai'i[d]									
	Koke'e Up	headwater stream		4100	67.0	1.58E+02	1600	0.07	1.12
	Koke'e Down	stream		4100	--	--	1600	0.07	--
	Koke'e Tributary	stream		4100	--	--	1600	0.58	--
	WR @ dam	stream	Basalt, Oxisols	4100	67.0	7.76E+02	1142	0.37	0.36
	WR @ Po'o Koeha	stream		4100	67.0	1.14E+03	1142	0.54	0.56
	WR @ Powerhouse	stream		4100	67.0	1.52E+03	906	0.72	0.54
	WR @ ford	stream		4100	67.0	1.05E+03	546	0.50	0.90

Table DR1 (Continued)

Geochemical and Mo data for groundwater and river samples from the Hawaiian Islands and Critical Zone Observatories

Sample Location	Sample Name	Sample Type	Dominant rock type, soil order	Duration of weathering[a]	Discharge	Mo Discharge[b]	MAP[c]	Mo	δ^{98}Mo
				kyr	$m^3\ s^{-1}$	mol Mo yr^{-1}	mm yr^{-1}	nM	‰
Critical Zone Observatories (CZO)									
Eel River	S. fork Eel/Angelo Coast	stream	Siltstone, Inceptisols Alluvium/	0.8	1.90E+01	7.74E+02	1500	1.30	1.15
Reynolds	Johnston Draw	stream	Colluvium, Andisols/Mollisols	3.8	1.23E+00	7.44E+01	616	1.91	1.02
	Reynolds Mountain	stream	Alluvium/Colluvium, Andisols/Mollisols	3.8	1.23E+00	2.99E+01	803	0.77	1.08
Intensely Managed Landscapes	Clear Creek	stream	Alluvium, Alfisols/ Entisols/ Inceptisols/ Mollisols	5.0	--	--	889	1.98	--
Santa Catalina Mountains-Jimez River Basin	Marshall Gulch	stream	Schist/ Granite, Entisols/ Mollisols	12	1.91E+00	4.88E+03	800	81.11	0.5
Susquehanna Shale Hills	Rose Hill	stream	Shale, Alfisols/ Inceptisols/ Ultisols	15	1.16E-03	5.29E-03	1050	0.15	1.03
Boulder	Gordon Gulch	stream	Biotite-Gneiss, Inceptisols/ Alfisols/ Mollisols	20	7.00E-03	2.00E+00	519	9.04	1.36
Luquillo	Mamayes	stream	Volcani-clastic, Ultisols	55	1.59E+00	3.05E+01	4200	0.61	1.44
	Icacos	stream	Grano-	125	3.80E-01	4.58E+00	3080	0.29	0.61

			diorite, Inceptisols						
	Guaba Ridge	headwater stream	Grano-diorite, Inceptisols	125	1.30E-02	1.20E-01	3080	0.38	1.24
Southern Sierra	Providence Creek	stream	Granite, Alfisols/ Entisols/ Inceptisols	142	1.80E-02	3.95E-01	1200	0.70	1.16
Calhoun	Weir 3	stream	Igneous-felsic intrusive, Ultisols	1300	--	--	1300	0.15	--
	Weir 4	stream	Igneous-felsic intrusive, Ultisols	1300	1.00E-03	4.63E-03	1300	0.62	1.35
	Holcomb	stream	Igneous-felsic intrusive, Ultisols	1300	1.00E-03	6.33E-02	1300	2.01	0.92

[a] At locations where duration of weathering data does not exist, approximate duration was estimated using published denudation rates, average soil depths, and assumed soil densities (Lybrand et al., 2011; Dosseto et al., 2012; Buss et al., 2017; Pett-Ridge et al., 2009; Leithold et al., 2006; Dethier et al., 2012; Foster et al., 2015; Holbrook et al., 2014; West et al., 2013; Bacon et al., 2012; Abaci and Papanicolaou, 2009; Patton, 2016).
[b] Annual Mo fluxes were calculated in areas where discharge data was available for the Hawaiian Islands (Schopka and Derry, 2012; Strauch et al., 2015) and the CZOs (Datasets: http://criticalzone.org/national/data/list-datasets/, accessed July 2017).
[c] MAP = mean annual precipitation
[d] WR = Waimea River

Methods

Groundwater samples were collected from 10 wells along the Kona Coast of the Big Island of Hawai'i. Samples PW1–PW4, PW7, and IW5 were collected from the Hualalai Resort and Kaupulehu Water Company in July 2015. The PW1–PW and PW7 samples were located at an elevation of 450 m and IW5 was located at an elevation of 260 m. The well depth ranged from 915 m to 1430 m, and all samples were collected using inlets located at 7 m below mean sea level. The Pu'u Wa'awa'a and Puu Lani samples were collected in collaboration with Napu'u Water, Inc. in July 2015 from well depths of 720 m and 735 m, respectively. The Ke'ei, Honokōhau, and Kalaoa wells were sampled in July 2016 with the Hawai'i Department of Water Supply with well depths of 410 m, 530 m, and 565 m, respectively. Each well was flushed for 30 min before water was collected in acid-washed bottles.

All samples were passed through 0.45-μm filters, and acidified to pH 2 with concentrated sub-boiled distilled HNO_3. Water samples were dried on a hot plate, refluxed twice in concentrated sub-boiled distilled HNO_3, and re-suspended in 5 mL of 0.5 M sub-boiled distilled HNO_3. Molybdenum concentrations were measured on a Thermo X-Series II Inductively Couple Plasma Mass Spectrometer (ICP-MS). A mixed-element solution standard was used for instrument calibration. Two USGS standards (BCR-2 and BHVO-2) were monitored for external reproducibility (BCR-2 = 258 ± 16 μg g^{-1} (n = 5); BHVO-2 = 4.43 ± 0.66 μg g^{-1} (n = 9)) and results agreed with published concentrations (BCR-2 = 248 ± 17 μg g^{-1}; BHVO-2 = 3.9 ± 2.3 μg g^{-1} (Li et al., 2014)). Procedural blanks for Mo were less than 5% of the lowest Mo concentration collected in the concentrated samples.

Molybdenum isotope measurements were performed on a Nu Plasma Multicollector (MC)-ICP-MS at Oregon State University using a ^{97}Mo-^{100}Mo double spike. The procedures for the double-spike and column chromatography are outlined in King et al., (2016). Isotope measurements are made relative to NIST SRM 3134 = +0.25‰ (Lot No.: 891307) and are reported in delta notation (δ^{98}Mo):

$$\delta^{98}Mo = \left(\left[\frac{\left(\frac{^{98}Mo}{^{95}Mo}\right)_{sample}}{\left(\frac{^{98}Mo}{^{95}Mo}\right)_{NIST\ SRM\ 3134}} - 1 \right] \cdot 1000 \right) + 0.25‰$$

Repeated measurements of an in-house standard (Alfa Aesar Specpure® Product No.: 35758 (Lot No.: 23-16504a)) yielded a δ^{98}Mo value of +0.09‰ ($2\sigma = \pm 0.12$‰, $n = 180$). Three USGS rock standards BCR-2 ($n = 72$), BHVO-2 ($n = 36$), and SDO-1 ($n = 45$) were also monitored and yielded δ^{98}Mo values of +0.24± 0.09‰, +0.21± 0.12‰, and +1.05± 0.13‰, in agreement with previously published results (BCR-2 = +0.22± 0.04‰, BHVO-2 = +0.22± 0.04‰, SDO-1 = +1.10± 0.16‰) (Goldberg et al., 2013; Liang et al., 2017).

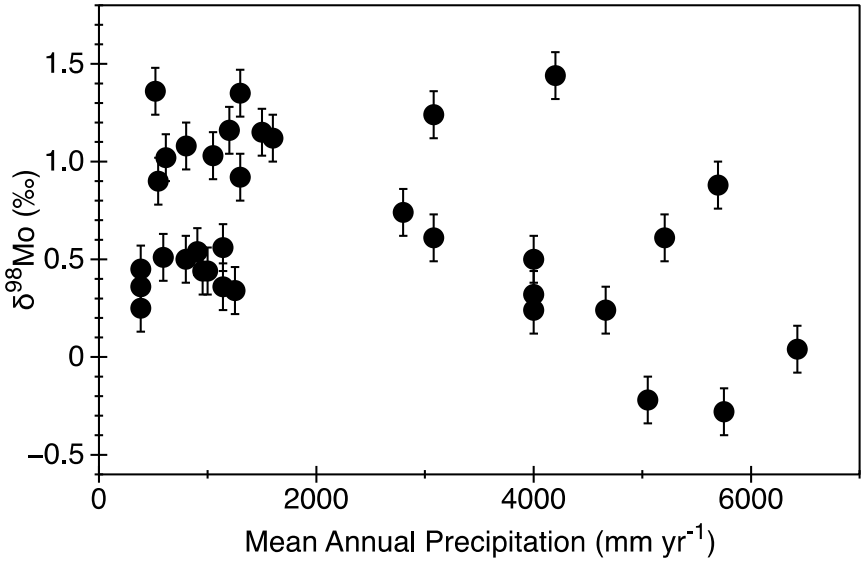

Figure DR1. δ^{98}Mo versus mean annual precipitation (mm yr^{-1}) for Hawaiian Islands and Critical Zone Observatories stream waters. There is no clear trend between MAP and δ^{98}Mo.

Table DR2
Subsurface soil Mo data from Hawai'i

Duration of weathering kyr	δ^{98}Mo ‰
0.3	0.05
10[a]	-0.2
10[a]	-0.01
10[a]	-0.28
10[a]	-0.38
10[a]	0.14
10[a]	0.06
10[a]	0.24
170	0.05
410[b]	-0.22
410[b]	-0.28
410[b]	-0.11
410[b]	0.05

[a] King et al. (2016)
[b] Siebert et al. (2015)

Table DR3

Published Mo data (Neely et al., 2018; Wang et al., 2015; Rahaman et al., 2014; Voegelin et al., 2012; Neubert et al., 2011; Pearce et al., 2010; Archer and Vance, 2008; Scheiderich et al., 2010)

Citation	Sample	Sample Type	Discharge $m^3\ s^{-1}$	Mo Discharge mol Mo yr^{-1}	Mo nM	$\delta^{98}Mo$[a] ‰	Water Discharge Reference[b]
Archer and Vance, 2008							
	Itchen	river	2.01E+03	2.53E+07	4.84	1.14	(Phillips et al., 2003)
	Kalix	river	2.01E+03	1.49E+09	7.74	1.00	
	Kalix	river	2.94E+04	2.19E+10	5.55	1.20	
	Kalix	river	2.94E+04	2.19E+10	5.03	1.05	
	Kalix	river	2.94E+04	2.19E+10	4.94	0.98	
	Kalix	river	2.94E+04	2.19E+10	4.91	1.11	
	Kalix	river	2.94E+04	2.19E+10	4.88	1.00	
	Nile	river	1.62E+04	1.66E+12	7.33	0.17	
	Nile	river	1.92E+02	1.97E+10	4.45	0.78	
	Nile	river	1.92E+02	1.97E+10	11.11	0.38	
	Nile	river	1.92E+02	1.97E+10	18.11	0.44	
	Nile	river	1.92E+02	1.97E+10	13.31	0.48	
	Nile	river	7.60E+03	7.80E+11	4.96	1.20	
	Nile	river	2.09E+05	2.15E+13	3.59	1.40	
	Nile	river	2.09E+05	2.15E+13	7.99	0.15	
	Nile	river	2.63E+03	2.70E+11	7.07	0.48	
	Volga	river	2.63E+03	1.17E+11	6.65	1.19	(Kroonenberg et al., 1997)
	Chang Jiang	river	2.63E+03	1.61E+11	16.71	0.95	
	Chang Jiang	river	2.63E+03	1.61E+11	16.81	0.65	
	Chang Jiang	river	2.63E+03	1.61E+11	17.71	0.89	
	Chang Jiang	river	2.63E+03	1.61E+11	17.11	0.83	
	Chang Jiang	river	2.63E+03	1.61E+11	15.91	0.90	
	Ottawa	river	2.63E+03	1.21E+10	2.17	2.25	
	Ottawa	river	2.63E+03	1.21E+10	2.00	2.40	
	Clear Creek	river	2.89E+02	1.36E+07	507.32	0.24	(USGS, 2018)
	Clear Creek	river	2.89E+02	1.36E+07	508.32	0.23	
	Clear Creek	river	2.89E+02	1.36E+07	511.32	0.24	
	Clear Creek	river	2.89E+02	1.36E+07	507.32	0.23	
	Brahamaputra	river	2.89E+02	1.48E+10	8.98	0.74	
	Amazon	river	2.89E+02	5.60E+10	4.34	0.57	
	Amazon	river	5.30E+00	1.03E+09	4.30	0.63	
Pearce et al., 2010							
	SE Iceland	river	1.75E+02	1.43E+04	2.59	-0.13	(Eiríksdóttir et al., 2014)
	SE Iceland	river	1.75E+02	4.23E+04	7.66	1.51	
	SE Iceland	river	1.75E+02	1.62E+04	2.94	0.07	
	SE Iceland	river	1.75E+02	7.17E+03	1.30	-0.01	
	SE Iceland	river	1.75E+02	8.61E+03	1.56	0.49	
	W Iceland	river	7.99E+01	7.11E+03	2.82	0.95	(Gannoun et al., 2006)
	W Iceland	river	7.99E+01	7.11E+03	2.82	0.95	
	W Iceland	river	7.99E+01	7.94E+03	3.15	0.90	
	W Iceland	river	7.99E+01	9.95E+03	3.95	0.96	
	W Iceland	river	7.99E+01	7.99E+03	3.17	1.00	
	W Iceland	river	7.99E+01	6.68E+03	2.65	0.60	
	W Iceland	river	7.99E+01	2.24E+04	8.91	0.44	
	W Iceland	river	7.99E+01	9.32E+03	3.70	0.71	
	W Iceland	river	7.99E+01	4.69E+03	1.86	0.39	
	W Iceland	river	7.99E+01	7.69E+03	3.05	0.63	
	W Iceland	river	7.99E+01	2.02E+03	0.80	1.77	
	W Iceland	river	7.99E+01	4.38E+03	1.74	1.10	
Scheiderich et al., 2010							
	Susquehanna	river	1.10E+03	9.76E+04	2.81	1.02	

Neubert et al., 2011							
	Chang Jiang	China	1.42E+03	8.72E+10	9.01	1.22	(Archer and Vance, 2008)
	Chang Jiang	China	1.42E+03	8.72E+10	13.01	1.11	
	Entlebuch	Switzerland	2.94E+04	4.64E+08	1.79	0.46	(Pappas, 2014)
	Entlebuch	Switzerland	2.94E+04	4.64E+08	1.11	0.36	
	Entlebuch	Switzerland	1.45E+01	2.29E+05	1.65	0.35	
	Entlebuch	Switzerland	1.45E+01	2.29E+05	0.90	0.16	
	Entlebuch	Switzerland	1.45E+01	2.29E+05	0.71	0.14	
	Entlebuch	Switzerland	1.45E+01	2.29E+05	0.53	0.27	
	Entlebuch	Switzerland	1.45E+01	2.29E+05	2.95	1.25	
	Entlebuch	Switzerland	1.45E+01	2.29E+05	2.45	1.50	
	Entlebuch	Switzerland	1.45E+01	2.29E+05	2.71	1.29	
	Entlebuch	Switzerland	1.45E+01	2.29E+05	2.69	1.60	
	Entlebuch	Switzerland	1.45E+01	2.29E+05	1.97	1.09	
	Entlebuch	Switzerland	1.45E+01	2.29E+05	2.34	1.01	
	Entlebuch	Switzerland	1.45E+01	2.29E+05	2.49	1.21	
	Aare	Switzerland	1.45E+01	2.29E+05	5.09	1.22	(Person et al., 2014)
	Aare	Switzerland	1.45E+01	2.29E+05	5.69	1.13	
	Aare	Switzerland	3.50E+01	5.52E+05	5.82	1.34	
	Aare	Switzerland	3.50E+01	5.52E+05	6.94	1.04	
	Aare	Switzerland	3.50E+01	5.52E+05	7.18	1.05	
	Aare	Switzerland	3.50E+01	5.52E+05	9.13	0.90	
	Aare	Switzerland	3.50E+01	5.52E+05	2.08	1.90	
	Sikkim	India	3.50E+01	1.38E+07	139.09	0.59	(Mondal and Islam, 2017)
	Sikkim	India	3.50E+01	1.38E+07	43.03	0.56	
	Sikkim	India	1.42E+03	5.63E+08	90.06	0.57	
	Sikkim	India	1.42E+03	5.63E+08	44.03	0.66	
Voegelin et al., 2012							
	Malaval	river	--	--	8.44	1.13	
	Malaval	river	--	--	3.13	0.72	
	Sejallieres	river	--	--	2.08	1.07	
	Sejallieres	river	--	--	1.77	1.02	
	Malaval	river	--	--	0.21	0.83	
	Malaval	river	--	--	0.42	0.67	
	Malaval	river	--	--	1.56	0.73	
	Malaval	river	--	--	1.25	0.65	
	Malaval	river	--	--	1.25	0.55	
	Malaval	river	--	--	1.56	0.58	
	Malaval	river	--	--	0.73	0.91	
	Malaval	river	--	--	1.46	0.67	
Rahaman et al., 2014							
	Narmada	river	1.45E+03	1.96E+05	4.30	0.40	
	Tapi	river	4.89E+02	9.41E+04	6.10	1.10	
Wang et al., 2015							
	Xijang	river	1.68E+02	4.93E+04	9.32	1.34	
	Xijang	river	2.26E+02	7.45E+04	10.46	1.29	
	Xijang	river	8.60E+02	2.16E+05	7.95	1.43	
	Xijang	river	1.47E+04	2.00E+06	4.32	1.55	
	Xijang	river	9.60E+02	1.69E+05	5.59	1.56	
	Xijang	river	1.45E+03	2.53E+05	5.53	1.50	
	Xijang	river	8.20E+02	1.37E+05	5.28	1.49	
	Xijang	river	3.80E+02	9.34E+04	7.79	1.43	
	Xijang	river	1.45E+03	3.45E+05	7.55	1.42	
	Xijang	river	3.90E+02	8.36E+04	6.80	1.49	
	Xijang	river	2.10E+02	4.88E+04	7.37	1.52	
	Xijang	river	8.60E+02	2.03E+05	7.49	1.39	
	Xijang	river	2.70E+02	6.24E+04	7.33	1.39	
	Xijang	river	2.36E+02	5.48E+04	7.36	1.41	

	Xijang	river	2.65E+02	6.27E+04	7.50	1.49	
	Xijang	river	2.65E+02	6.10E+04	7.30	1.42	
	Xijang	river	5.60E+02	1.23E+05	6.98	1.47	
	Huanghe	river	1.59E+03	4.90E+06	97.96	0.42	
	Huanghe	river	3.81E+02	1.06E+06	88.16	0.50	
	Huanghe	river	7.99E+02	2.15E+06	85.45	0.53	
	Huanghe	river	4.13E+02	1.16E+06	89.46	0.55	
	Huanghe	river	4.77E+02	1.19E+06	79.45	0.63	
	Huanghe	river	7.16E+02	2.53E+06	112.07	0.49	
	Huanghe	river	2.44E+02	8.46E+04	11.01	0.62	
	Huanghe	river	2.04E+02	6.15E+05	95.66	0.61	
	Huanghe	river	2.78E+02	7.81E+05	89.16	0.60	
	Huanghe	river	1.13E+03	3.29E+06	92.26	0.47	
	Huanghe	river	8.40E+02	3.10E+06	117.07	0.53	
	Huanghe	river	1.58E+03	6.13E+06	123.08	0.34	
	Huanghe	river	3.13E+02	1.09E+06	110.07	0.37	
	Huanghe	river	2.18E+02	6.94E+05	101.06	0.40	
	Huanghe	river	--	--	82.95	0.54	
Neely et al., 2018[c]							
	AB-2	groundwater	2.16E+03	2.25E+04	0.33	0.29	(Pearce et al., 2010)
	LUD-4	groundwater	2.16E+03	1.03E+05	1.52	1.12	
	LUD-2	groundwater	2.16E+03	3.84E+04	0.57	0.39	
	LUD-3	groundwater	2.16E+03	4.04E+04	0.59	0.39	
	Garoslind	groundwater	2.16E+03	4.45E+04	0.65	0.47	
	Hverdjallasgja	groundwater	2.16E+03	4.85E+04	0.71	0.38	
	Vagafloi	groundwater	2.16E+03	5.52E+04	0.81	0.33	
	Peistareykir-vatnsbol	groundwater	2.16E+03	1.20E+04	0.18	0.68	
	Krossdalur	groundwater	2.16E+03	1.23E+04	0.18	0.00	
	Fjoll-lind	groundwater	2.16E+03	1.42E+04	0.21	-0.08	
	Fjoll-vatnsbol	groundwater	2.16E+03	7.00E+03	0.10	0.17	
	Lon	groundwater	2.16E+03	1.73E+04	0.26	0.06	
	PR-8	groundwater	2.16E+03	6.60E+03	0.10	-0.15	
	PR-16	groundwater	2.16E+03	1.29E+04	0.19	-0.04	

[a] Data has been normalized to NIST 3134 = +0.25‰

[b] Water discharge reference is only listed if it is different from cited Mo study from which data was compiled. Samples from the same river have the same water discharge citation.

[c] Groundwater samples classified as < 10°C (not hydrothermally altered). Groundwater discharge was estimated for the entire island assuming submarine groundwater was 40% of riverine discharge reported in Pearce et al., 2010.

Hawaiian groundwater mixing model

In Hawai'i, groundwater exists as a freshwater basal lens overlying seawater that has permeated into the bedrock, and there is potential for this input to affect our groundwater results. Seawater Mo is isotopically heavy (δ^{98}Mo = +2.3± 0.15‰), Barling et al., 2001; Siebert et al., 2003) and can contribute to the observed heavy groundwater δ^{98}Mo. Schopka and Derry (2012) measured the influence of seawater on groundwater samples collected in the Kona region of Hawai'i and determined that seawater contamination accounted for < 10% of their groundwater samples. We can explore the possible effect of seawater with a simple mixing model, whereby seawater has a Mo concentration of 111 nM and a δ^{98}Mo value of +2.3‰ and the primary mineral dissolution endmember (basalt) has a Mo concentration of ~ 35 nM (average groundwater Mo concentration corrected for 10% seawater intrusion) and a δ^{98}Mo value of +0.14‰ (± 0.17‰, average Hawaiian basalt). In this scenario, mixing between the deep weathering and seawater endmembers does not account for all groundwater samples (Fig. DR2).

To calculate an average δ^{98}Mo value for the dissolved Mo leaching from soils we first calculated the total Mo groundwater flux could be derived from soils. This calculation was based on the total groundwater flux reported in Table 2 (Hawai'i, "rest of island") of Schopka and Derry (2012) and the average Mo concentration in groundwater from this study (41.3 nM). Next, we compared this value to the soil Mo leaching flux for the Kona coast, reported in King et al., (2016) (MAP = 2100 mm yr^{-1}) and calculated that 5% of the total groundwater flux comes from shallow, soil-derived flowpaths leaching into groundwater. We set up an isotope mass balance model to calculate a δ^{98}Mo value for this soil leach solution assuming that the average groundwater δ^{98}Mo value (+0.39±0.17‰) was a function of dissolved Mo leaching from soils, seawater intrusion (+2.3‰), and Hawaiian basalt (+0.14±0.17‰). This allows us to calculate a δ^{98}Mo soil leaching value of +0.82‰, which can potentially explain why we see a slightly heavier groundwater δ^{98}Mo value relative to bedrock (Fig. DR2).

Another possible explanation for the slightly heavier Mo signature in groundwater is the incongruent dissolution of mineral phases. However, the Mo isotopic composition of individual primary minerals in Hawaiian basalts is not known, and other studies from both basalts and granites have shown that the incongruent dissolution of Mo phases may lead to δ^{98}Mo values that deviate from bedrock (Voegelin et al., 2012, 2014). For example, the fractional crystallization of light Mo into hornblende and biotite led to these mineral phases being ~ 0.6‰ lighter than bulk rock, which requires other Mo phases to be isotopically heavy (Voegelin et al., 2014). Moreover, sulfide minerals—which are easily dissolved under oxidizing environments—are a major host phase for Mo and possess a wide variation in δ^{98}Mo values that range from -1.4‰ to +2.5‰ (Breillat et al., 2016). Although sulfides within Hawaiian basaltic glass contain low concentrations of Mo (2.6 ppm) (Greaney et al., 2017), if these phases are enriched in heavy isotopes there is potential for groundwater δ^{98}Mo to reflect the preferential dissolution of Mo from sulfide phases.

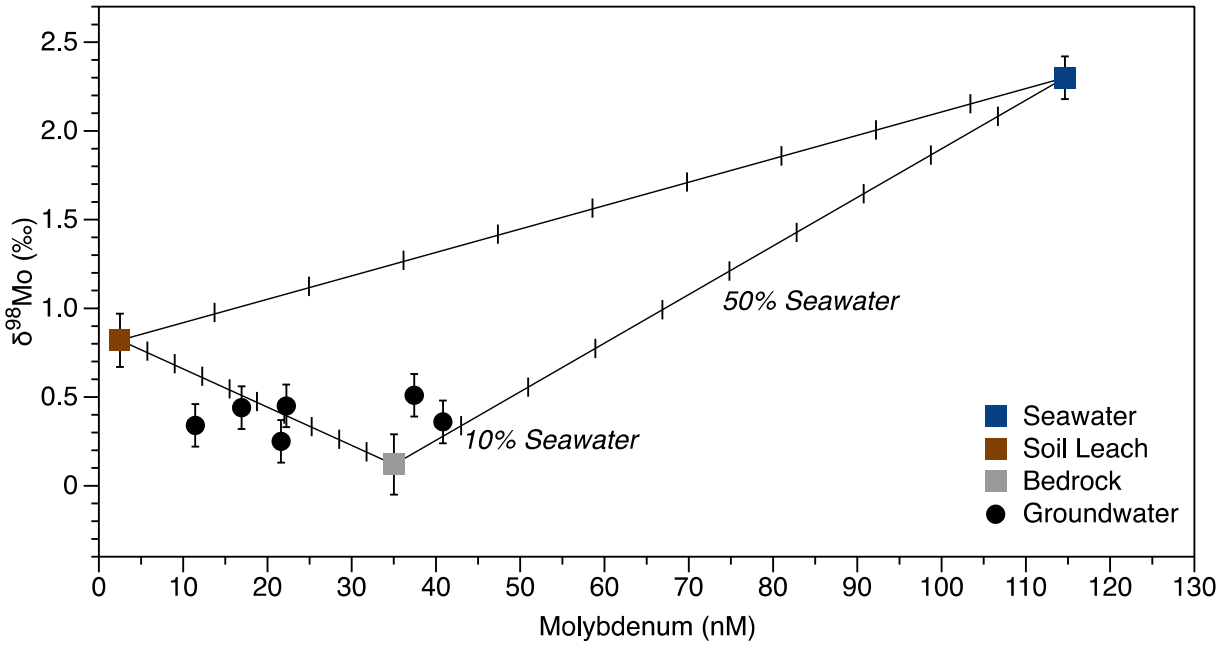

Figure DR2. Mixing plot between seawater, Hawaiian basalt, and Mo leaching from soils. Groundwater samples do not fall on a linear mixing plot (solid lines, tick marks represent 10% endmember intervals), suggesting that both fractionation in soils and seawater input may affect δ^{98}Mo signatures. The dominant endmember in groundwater seems to be Mo entering the dissolved phase through the initial stages of chemical weathering with an unfractionated δ^{98}Mo value relative to bedrock. Error on the δ^{98}Mo data for groundwater and seawater refers to the external reproducibility of in-house standard (± 0.12‰), and error on the soil leach δ^{98}Mo (± 0.15‰) is propagated from the parameters included in the isotope mass balance. Basalt δ^{98}Mo is an average of data reported in Siebert et al., (2015), King et al., (2016), and Liang et al., (2017).

Supplemental References

Abaci, O., and Papanicolaou, A.N.T., 2009, Long-term effects of management practices on water-driven soil erosion in an intense agricultural sub-watershed: monitoring and modelling: Hydrological Processes, v. 23, p. 2818–2837, doi: 10.1002/hyp.

Archer, C., and Vance, D., 2008, The isotopic signature of the global riverine molybdenum flux and anoxia in the ancient oceans: Nature Geoscience, v. 1, p. 597–600, doi: 10.1038/ngeo282.

Bacon, A.R., Richter, D., Bierman, P.R., and Rood, D.H., 2012, Coupling meteoric 10be with pedogenic losses of 9be to improve soil residence time estimates on an ancient North American interfluve: Geology, v. 40, p. 847–850, doi: 10.1130/G33449.1.

Barling, J., Arnold, G.L., and Anbar, A.D., 2001, Natural mass-dependent variations in the isotopic composition of molybdenum: Earth and Planetary Science Letters, v. 193, p. 447–457, doi: 10.1016/S0012-821X(01)00514-3.

Breillat, N., Guerrot, C., Marcoux, E., and Négrel, P., 2016, A new global database of δ98Mo in molybdenites: A literature review and new data: Journal of Geochemical Exploration, v. 161, p. 1–15, doi: 10.1016/j.gexplo.2015.07.019.

Buss, H.L., Chapela Lara, M.M., Moore, O.W., Kurtz, A.C., Schulz, M.S., and White, A.F., 2017, Lithological influences on contemporary and long-term regolith weathering at the Luquillo Critical Zone Observatory: Geochimica et Cosmochimica Acta, v. 196, p. 224–251, doi: 10.1016/j.gca.2016.09.038.

Dethier, D.P., Birkeland, P.W., and McCarthy, J.A., 2012, Using the accumulation of CBD-extractable iron and clay content to estimate soil age on stable surfaces and nearby slopes, Front Range, Colorado: Geomorphology, v. 173–174, p. 17–29, doi: 10.1016/j.geomorph.2012.05.022.

Dosseto, A., Buss, H.L., and Suresh, P.O., 2012, Rapid regolith formation over volcanic bedrock and implications for landscape evolution: Earth and Planetary Science Letters, v. 337–338, p. 47–55, doi: 10.1016/j.epsl.2012.05.008.

Foster, M.A., Anderson, R.S., Wyshnytzky, C.E., Ouimet, W.B., and Dethier, D.P., 2015, Hillslope lowering rates and mobile-regolith residence times from in situ and meteoric 10Be analysis, Boulder Creek Critical Zone Observatory, Colorado: Bulletin of the Geological Society of America, v. 127, p. 862–878, doi: 10.1130/B31115.1.

Goldberg, T., Gordon, G., Izon, G., Archer, C., Pearce, C.R., McManus, J., Anbar, A.D., and Rehkämper, M., 2013, Resolution of inter-laboratory discrepancies in Mo isotope data: an intercalibration: Journal of Analytical Atomic Spectrometry, v. 28, p. 724, doi: 10.1039/c3ja30375f.

Greaney, A.T., Rudnick, R.L., Helz, R.T., Gaschnig, R.M., Piccoli, P.M., and Ash, R.D., 2017, The behavior of chalcophile elements during magmatic differentiation as observed in Kilauea Iki lava lake Hawaii: Geochimica et Cosmochimica Acta, v. 210, p. 71–96, doi: 10.1016/j.gca.2017.04.033.

Holbrook, W.S., Riebe, C.S., Elwaseif, M., Hayes, J.L., Basler-reeder, K., Harry, D.L., Malazian, A., Dosseto, A., Hartsough, P.C., and Hopmans, J.W., 2014, Geophysical constraints on deep weathering and water storage potential in the Southern Sierra Critical Zone Observatory: Earth Surface Processes and Landforms, v. 380, p. 366–380, doi: 10.1002/esp.3502.

King, E.K., Thompson, A., Chadwick, O.A., and Pett-Ridge, J.C., 2016, Molybdenum sources and isotopic composition during early stages of pedogenesis along a basaltic climate transect: Chemical Geology, doi: 10.1016/j.chemgeo.2016.01.024.

Leithold, E.L., Blair, N.E., and Perkey, D.W., 2006, Geomorphologic controls on the age of particulate organic carbon from small mountainous and upland rivers: Global Biogeochemical Cycles, v. 20, p. 1–11, doi: 10.1029/2005GB002677.

Li, J., Liang, X.R., Zhong, L.F., Wang, X.C., Ren, Z.Y., Sun, S.L., Zhang, Z.F., and Xu, J.F., 2014, Measurement of the Isotopic Composition of Molybdenum in Geological Samples by MC-ICP-MS using a Novel Chromatographic Extraction Technique: Geostandards and Geoanalytical Research, v. 38, p. 345–354, doi: 10.1111/j.1751-908X.2013.00279.x.

Liang, Y.H., Halliday, A.N., Siebert, C., Fitton, J.G., Burton, K.W., Wang, K.L., and Harvey, J., 2017, Molybdenum isotope fractionation in the mantle: Geochimica et Cosmochimica Acta, v. 199, p. 91–111, doi: 10.1016/j.gca.2016.11.023.

Lybrand, R., Rasmussen, C., Jardine, A., Troch, P., and Chorover, J., 2011, Applied Geochemistry The effects of climate and landscape position on chemical denudation and mineral transformation in the Santa Catalina mountain critical zone observatory: Applied Geochemistry, v. 26, p. S80–S84, doi: 10.1016/j.apgeochem.2011.03.036.

Neely, R.A., Gislason, S.R., Ólafsson, M., McCoy-West, A.J., Pearce, C.R., and Burton, K.W., 2018, Molybdenum isotope behaviour in groundwaters and terrestrial hydrothermal systems, Iceland: Earth and Planetary Science Letters, v. 486, p. 108–118, doi: 10.1016/J.EPSL.2017.11.053.

Neubert, N., Heri, A.R., Voegelin, A.R., Nägler, T.F., Schlunegger, F., and Villa, I.M., 2011, The molybdenum isotopic composition in river water: Constraints from small catchments: Earth and Planetary Science Letters, v. 304, p. 180–190, doi: 10.1016/j.epsl.2011.02.001.

Patton, N.R., 2016, Topographic Controls on Total Mobile Regolith and Total Soil Organic Carbon in Complex Terrain: Idaho State University.

Pearce, C.R., Burton, K.W., Pogge von Strandmann, P.A.E., James, R.H., and Gíslason, S.R., 2010, Molybdenum isotope behaviour accompanying weathering and riverine transport in a basaltic terrain: Earth and Planetary Science Letters, v. 295, p. 104–114, doi: 10.1016/j.epsl.2010.03.032.

Pett-Ridge, J.C., Derry, L.A., and Kurtz, A.C., 2009, Sr isotopes as a tracer of weathering processes and dust inputs in a tropical granitoid watershed, Luquillo Mountains, Puerto Rico: Geochimica et Cosmochimica Acta, v. 73, p. 25–43, doi: 10.1016/j.gca.2008.09.032.

Rahaman, W., Goswami, V., Singh, S.K., and Rai, V.K., 2014, Molybdenum isotopes in two Indian estuaries: Mixing characteristics and input to oceans: Geochimica et Cosmochimica Acta, v. 141, p. 407–422, doi: 10.1016/j.gca.2014.06.027.

Scheiderich, K., Helz, G.R., and Walker, R.J., 2010, Century-long record of Mo isotopic composition in sediments of a seasonally anoxic estuary (Chesapeake Bay): Earth and Planetary Science Letters, v. 289, p. 189–197, doi: 10.1016/j.epsl.2009.11.008.

Schopka, H.H., and Derry, L.A., 2012, Chemical weathering fluxes from volcanic islands and the importance of groundwater: The Hawaiian example: Earth and Planetary Science Letters, v. 339–340, p. 67–78, doi: 10.1016/j.epsl.2012.05.028.

Siebert, C., Nägler, T.F., von Blanckenburg, F., and Kramers, J.D., 2003, Molybdenum isotope records as a potential new proxy for paleoceanography: Earth and Planetary Science Letters, v. 211, p. 159–171, doi: 10.1016/S0012-821X(03)00189-4.

Siebert, C., Pett-Ridge, J.C., Opfergelt, S., Guicharnaud, R.A.A., Halliday, A.N.N., and Burton, K.W.W., 2015, Molybdenum isotope fractionation in soils: Influence of redox conditions, organic matter, and atmospheric inputs: Geochimica et Cosmochimica Acta, v. 162, p. 1–24, doi: 10.1016/j.gca.2015.04.007.

Strauch, A.M., MacKenzie, R.A., Giardina, C.P., and Bruland, G.L., 2015, Climate driven changes to rainfall and streamflow patterns in a model tropical island hydrological system: Journal of Hydrology, v. 523, p. 160–169, doi: 10.1016/j.jhydrol.2015.01.045.

Voegelin, A.R., Nägler, T.F., Pettke, T., Neubert, N., Steinmann, M., Pourret, O., and Villa, I.M., 2012, The impact of igneous bedrock weathering on the Mo isotopic composition of stream waters: Natural samples and laboratory experiments: Geochimica et Cosmochimica Acta, v. 86, p. 150–165, doi: 10.1016/j.gca.2012.02.029.

Voegelin, A.R., Pettke, T., Greber, N.D., Von Niederhäusern, B., and Nägler, T.F., 2014, Magma differentiation fractionates Mo isotope ratios: Evidence from the Kos Plateau Tuff (Aegean Arc): Lithos, v. 190–191, p. 440–448, doi: 10.1016/j.lithos.2013.12.016.

Wang, Z., Ma, J., Li, J., Wei, G., Chen, X., Deng, W., Xie, L., Lu, W., and Zou, L., 2015, Chemical weathering controls on variations in the molybdenum isotopic composition of river water: Evidence from large rivers in China: Chemical Geology, v. 410, p. 201–212, doi: 10.1016/j.chemgeo.2015.06.022.

West, N., Kirby, E., Bierman, P., Slingerland, R., Ma, L., Rood, D., and Brantley, S., 2013, Regolith production and transport at the Susquehanna Shale Hills Critical Zone Observatory, part 2: Insights from meteoric ^{10}Be: Journal of Geophysical Research: Earth Surface, v. 118, p. 1877–1896, doi: 10.1002/jgrf.20121.

Site	Latitude	Longitude
Hawaii		
Puu Lani Ranch Well	19.81	-155.83
Puu Waa Waa Ranch Well	19.78	-155.84
Pololu Stream 1	20.22	-155.76
Pololu Stream 2	20.21	-155.74
WP 87 Stream	20.22	-155.77
PW1 well	19.81	-155.97
PW3 well	19.81	-155.97
PW4 well	19.81	-155.97
PW7 well	19.81	-155.97
IW5 well	19.81	-155.97
Honolii	19.77	-155.16
Kapue	19.79	-155.15
Kolekole	19.85	-155.17
Umauma	19.89	-155.18
Manoloa	19.96	-155.25
Makahiloa	19.93	-155.21
Pahale	19.94	-155.23
Manowaiopae	19.96	-155.25
Maui		
MCG site 3	20.81	-156.25
MCG site 5	20.81	-156.24
Kauai		
Waimea River at dam	22.07	-159.65
Waimea River at ford	21.97	-159.66
Waimea River at powerhouse	22.04	-159.64
Waimea River at Po'o Koeha	22.07	-159.65
Koke'e Upstream	22.12	-159.65
Koke'e Downstream	22.11	-159.66
Koke'e Tributary	22.13	-159.64